Proton Transfer in $(HCOOH)_2$: An IR High-Resolution Spectroscopic Study of the Antisymmetric C−O Stretch†

Markus Ortlieb and Martina Havenith*

Department of Physical Chemistry II, Ruhr-University Bochum, Universitätsstrasse 150, D-44780 Bochum, Germany

Received: January 29, 2007; In Final Form: April 25, 2007

We report the fully analyzed high-resolution spectrum of the carboxylic acid dimer $(HCOOH)_2$ in the gas phase. High-resolution IR spectra in the region of the antisymmetric C−O stretch vibration have been recorded at 1221.0−1226.7 cm^{-1}. The data could be fit within experimental uncertainty to a rigid rotor Watson *S*-reduced Hamiltonian. The vibrational frequency of the C−O vibration is 1225.3430(3) cm^{-1}. On the basis of the measurement of a tunneling splitting of 0.0158(4)cm^{-1} for the lower state and 0.0100(3) cm^{-1} for the upper state, we determine a proton-transfer time of 1.0 and 1.7 ns for the ground and the vibrationally excited state, respectively.

1. Introduction

Because of the exceptional importance of hydrogen bonds in biology and chemistry, a detailed investigation of the structure and dynamics of hydrogen bonds has attracted the attention of several experimental and theoretical groups. Double hydrogen-bonded systems play a crucial role in that they serve as model systems for the understanding of DNA base pairs. Moreover, multiple proton transfer in hydrogen-bonded systems is one of the most fundamental processes in biology and chemistry. The smallest organic complex serving as a prototype for multiple proton transfer is the formic acid dimer. Formic acid dimerizes like all carboxylic acids with two hydrogen bonds forming a planar eight-numbered ring between the two monomers. The study of the double proton transfer in the hydrogen-bonded dimer of formic acid has therefore served as a benchmark system for theorists for more than 50 years.

A. The Structure of Formic Acid Dimer. Early theoretical work on formic acid dimer (FAD) was concerned with the dimer equilibrium geometry and the electronic structure (see, for example, refs 1−4). Ab initio molecular orbital studies on the structure of formic acid dimer in 1984 agreed very well with the experimental structures as determined by electron diffraction.[5] Because of the importance of the double proton transfer of FAD as a prototype for multiple proton transfer reactions, several theoretical studies are published in the literature.[6] Rotational constants for formic acid dimer were obtained by high-resolution spectroscopy of $(DCOOH)_2$[7] and by femtosecond degenerate four-wave mixing experiments by Matylisky et al.[8] The best agreement is obtained with the pure ab initio predictions by Neuheusser et al.[9] using MP2 with counterpoint-wise correction for basis set superposition error and a TZ2P basis set. These calculations predict an O···O distance of 2.672 Å. DFT calculations[10] yield a smaller O···O distance of 2.6451 Å with a hence increased B value. The MP2 calculations by Kim[11] and the extended molecular mechanics calculation slightly overestimated O···O (2.707 Å), thereby yielding a slightly too small B value. The first experimental structure of the dimer was determined by electron diffraction measurements, which yielded an O···O distance of 2.696 Å.

Rotational constants for $(HCOOH)_2$ were deduced by Matylitsky et al.[8] using time-resolved fs degenerate four-wave mixing. A comparison with rotational constants from $(DCOOH)_2$,[7] via model structures based upon the results of ab initio calculations[12] yield an agreement within (0.1−0.6%). Both sets of rotational parameters disagree with the rotational parameters as predicted for a structure as proposed by electron diffraction studies.[5] Whereas the deviation from this very early study is small, the deviation is still beyond the estimated experimental uncertainty.

B. Proton Transfer Tunneling of Formic Acid Dimer. Carboxylic dimers are well-suited systems to study coherent proton tunneling processes because they provide two identical hydrogen bonds. For the most stable and simplest prototypes of these such as formic acid dimer, the displacement of the protons can be described by a multidimensional potential involving a double well with two equal potential minima. The barriers are high compared to the zero-point energy because these species are bound by two cooperatively strengthened hydrogen bonds. Quantum mechanically, the two protons that are involved in the hydrogen bonds can tunnel even when the transition barrier is much higher than their kinetic energy, requiring a quantum mechanical description. The proton transfer gives rise to a splitting of each rotational−vibrational state into two states (E_l and E_u), which are separated by $\Delta E = h\nu_{\text{tunneling}}$ with $\nu_{\text{tunneling}}$ describing the tunneling frequency for double proton transfer. Because of the great sensitivity of the splitting to the shape of the potential surface, an accurate prediction of tunneling splittings even for this small prototype system remains still a challenge for theory.

It has been speculated whether the coherent proton transfer can be described as a synchronous concerted double proton transfer or whether at the start an asynchronous movement such as a step-by-step process will be the adequate picture. Most theoretical calculations propose for the carboxylic dimer a synchronous concerted proton transfer process, where the two monomers will first approach each other, before tunneling can occur. In 1995, Kim reported a direct dynamics calculation.[11] It was proposed that the two monomers first approach each

† Part of the "Roger E. Miller Memorial Issue".

* Corresponding author. E-mail: martina.havenith@ruhr-uni-bochum.de.

10.1021/jp070763+ CCC: $37.00
Published on Web 06/07/2007

other, thereby decreasing the barrier for tunneling before proton transfer takes place. At the transition state, the structure of formic acid dimer changes from C_{2h} to D_{2h} symmetry. The tunneling splitting ΔE depends sensitively on the barrier height and on the barrier width. In the work by Shida et al.,[13] a synchronous concerted double proton transfer is predicted to be the major mode of the reaction, which is confirmed in a recent molecular dynamics calculation by Wolf et al.[14] In a more recent calculation by Markwick et al., targeted molecular dynamics methods were implemented in the framework of Car-Parinello molecular dynamics to study the nature of the double proton transfer, predicting a concerted proton transfer reaction.[15] A different mechanism for interconversion of the hydrogen-bonded dimers of formic acid dimer (quantum entanglement) was proposed by Fillaux.[16]

Predictions of the proton transfer tunneling splitting cover several orders of magnitude: Chang et al. predicted a proton transfer tunneling splitting of 0.3 cm^{-1} corresponding to a proton transfer time of $\tau = 55$ ps.[17] In 1991, Shida, Barbara, and Almlöf used a reaction surface Hamiltonan to predict the proton transfer barrier for FAD.[13] Using MCPF (modified couple pair functionals), they predicted a tunneling splitting of 0.004 cm^{-1} ($\tau = 4.2$ ns). Molecular dynamics calculations by Ushiyama and Takatsuka[18] yielded transfer times of less than 150 fs, which is 3−4 orders of magnitude faster than any of the previous calculations. It should be noted that, in a paper by Vener et al.[19] using a similar approach as Shida et al., a tunneling splitting of 0.3 cm^{-1} instead of 0.004 cm^{-1} was calculated.

The first and so far only experimental study giving information on the tunneling splitting in formic acid dimer has been carried out in 2002 by Madeja and Havenith,[7] who reported the measurement of the tunneling splitting in $(DCOOH)_2$. It is assumed that the measured tunneling splitting is not much affected by the outside deuteration, thereby yielding valuable information on the size of the proton transfer tunneling splitting for this important prototype system. In our previous study, the size of the tunneling could not be determined unambiguously, yielding in the ground state a tunneling splitting of either 0.00286(25) or 0.0125(3) cm^{-1}.

In 2004, Tautermann et al.[20] predicted a ground-state tunneling splitting of 0.0022 cm^{-1} for formic acid dimer (which is equal to the predicted ground state tunneling splitting of benzoic acid dimer). They apply a semiclassical method to determine the ground state tunneling splitting of various carboxylic acid derivative dimers. The energy barriers were calculated using hybrid densiy functional theory (B3LYP) and compared to the result of a high-level method (MP2).

Smedarchina[21] reported direct dynamics calculations of tunneling splittings due to double proton transfer in formic and benzoic acid dimers based on instanton techniques. They predicted zero-point splittings of 375 MHz (0.012509 cm^{-1}) for $(DCOOH)_2$ and 1107 MHz (0.036926 cm^{-1}) for benzoic acid dimer.

Milnikov, Kühn, and Nakamura[22] applied the instanton theory to the calculation of vibrationally assisted tunneling splitting of the deuterated formic acid dimer $(DCOOH)_2$ with all degrees of freedom taken into account. Using density functional theory combined with coupled cluster level of quantum chemistry, the ground-state tunneling splitting is determined to be 0.0038 cm^{-1}. It was stated that the excitation mode may either enhance or suppress tunneling as compared to the ground state. For higher frequency modes, a rapid growth of the tunneling splitting is observed. At frequencies above 1000 cm^{-1}, the semiclassical solution becomes unstable, preventing a reliable prediction of the size of the tunneling splitting.

Luckhaus[23] has carried out fully coupled quantum dynamics calculations in up to six dimensions using potential energy hypersurfaces directly from hybrid density functional calculations with and without geometry relaxation. Using a calculated electronic barrier of 35.0 kJ/mol, the vibrational ground-state tunneling splitting is predicted to be 0.0013 cm^{-1}. Fully coupled rovibrational calculations demonstrate the compatibility of experimentally observed inertial defects with in-plane hydrogen exchange tunneling dynamics in formic acid dimer.

C. Infrared Vibrational Spectroscopy. An FTIR spectroscopic study of carboxylic acids in the gas phase including various isotopic forms of FAD has been reported by Marechal.[24] He recorded IR spectra in the frequency region from 500 to 4000 cm^{-1}, yielding detailed informations on IR band centers as well as their relative intensities. The vibrational band center of the C═O asymmetric stretch of FAD was measured at 1740 cm^{-1}. A later high-resolution study yielded two separate vibrational bands centered at 1738.5 and 1741.5 cm^{-1}.[25] However, because of the high density of lines in this frequency range, no definite assignment was possible. Anomalous isotope effects in the intensities of the ($\nu_{C=O}$) band of FAD[24] and Fourier transform (FT) studies of DCOOH[26] indicate a resonance between the C═O asymmetric stretch and combination bands, which considerably complicates the assignment of the gas-phase spectrum. Because of a lack of permanent dipole moment, no spectroscopic studies in the MW region are possible.

The first high-resolution spectroscopic measurements of FAD with fully resolved rotational−vibrational tunneling transitions were reported in 2002 by our group.[7] The C−O vibrational band of $(DCOOH)_2$ could be analyzed in terms of an asymmetric top rigid rotor Hamiltonian. The vibrational frequency of the C−O stretch in $(DCOOH)_2$ was determined to be 1244.8461(2) cm^{-1}, which deviated considerably from previous values for the band center as given by Wachs et al.[27] (1231.85 cm^{-1}). Previous values in the literature include Raman measurements as reported Bertie et al. (1230 ± 2 cm^{-1})[28] and IR studies by Millikan and Pitzer (1239 cm^{-1}).[29]

A complete FTIR spectrum of formic acid in the gas phase in a supersonic jet expansion with an experimental resolution of 0.5 cm^{-1} was reported by Georges et al.[30] In a paper by Florio et al.,[31] an overview including the theoretical modeling of the O−H stretch in carboxylic dimers is given. In general, large anharmonic effects and Fermi coupling result in a complicated band substructure in which the O−H stretch oscillator strength is spread over hundreds of wavenumbers.

The IR spectra of formic acid dimer, which was aggregated from (translationally) precooled monomers, showed an unexpected small red-shift in the O−H stretching region. The band was assigned to a free rather than a hydrogen bond O−H stretch, indicating the existence of a distinct structure for formic acid dimer. First, matrix isolation studies by the group of Sander suggested the existence of an open acyclic structure for FAD.[1] This has been confirmed by later measurements of formic acid dimer in helium nanodroplets.[12] Both studies clearly show the long-range preorientation of the two ultracold monomers before aggregation. Under these conditions, an acyclic instead of the expected double hydrogen-bonded structure was formed, with the first one corresponding to a local minimum in the potential surface. The thermodynamic most stable double hydrogen-bonded structure is not formed in the helium nanodroplet because a later reorientation would involve to pass over a

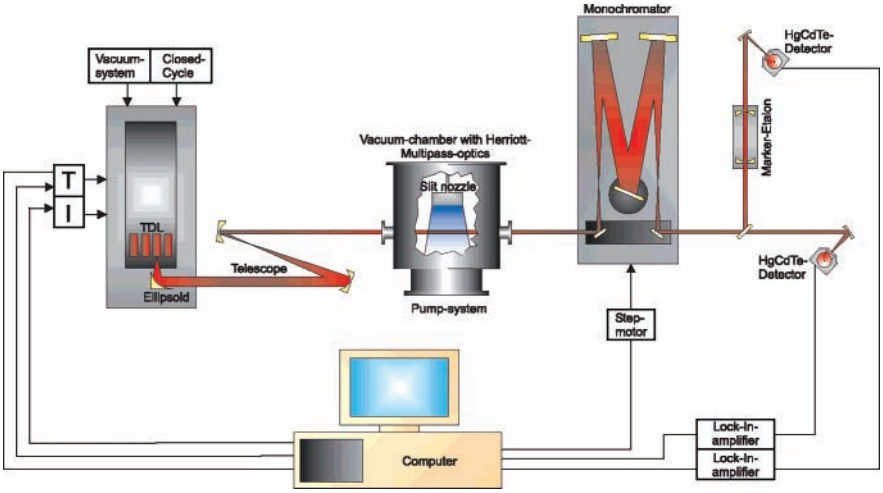

Figure 1. Experimental setup. Displayed is the lead salt diode laser spectrometer in combination with the supersonic jet expansion.

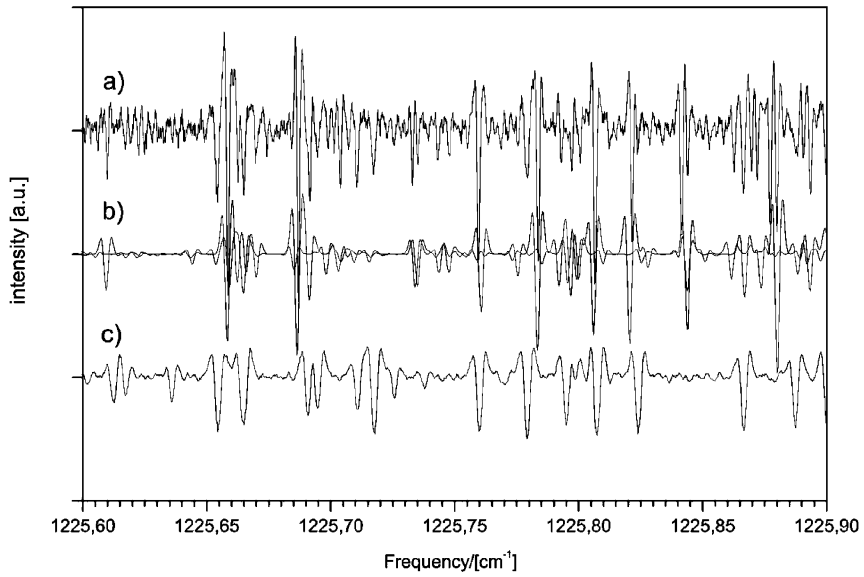

Figure 2. Displayed is a small part of the experimentally recorded spectrum, showing monomer and dimer transitions: We show (a) the measured spectra in the supersonic expansion including dimer and monomer transitions ($T = 15$ K), (b) the simulated dimer spectrum at $T = 15$ K, and (c) the IR spectrum at room temperature in a HCOOH/Ar mixture at a pressure of 650 mT. The difference in the intensity ratio of the monomer spectra in parts (a) and (c) can be explained by their different rotational temperatures. temperature conditions.

reaction barrier. At low temperatures (0.37 K in helium nanodroplets) and in an argon matrix at 40 K, the thermal energy is not high enough. However, when increasing the temperature, the energy barriers can be overcome and the double hydrogen-bonded dimer, corresponding to the global minimum is more populated.[1]

2. Experimental Results

The experiments were carried out using the infrared lead salt diode spectrometer set up in Bochum. The experimental setup is displayed in Figure 1. A more detailed description is given in refs 32,33. The clusters were formed in a supersonic jet expansion. The chamber is kept at a pressure of approximately 300 mTorr using a roots blower (Edwards EH 2600 m^3/h) backed by a second roots blower (Leybold 500 m^3/h) in combination with a mechanical pump (65 m^3/h). A 25:75% He−Ne mixture was used as carrier gas. By passing 1000 Torr through a bubbler that contained liquid HCOOH before the nozzle, we could form formic acid dimer in the supersonic expansion. We used two different types of nozzles: a planar cw slit nozzle [5 cm × 50 μm] and a pulsed planar nozzle [10 cm × 50 μm], which is opened for 2 ms and closed for 23 ms.

Using a Herriot multipass cell, the laser beam passes 32−36 times through the expansion before leaving the chamber, thereby increasing the overall absorption length to 190 cm. The absorption signal is recorded by a HgCdTe detector. The signal is detected using phase-sensitive detection with a lock-in detector at twice the frequency of the modulation of the laser current (2f modulation). Absolute frequency calibration was achieved by an Etalon with a 300 MHz free spectral range and by comparison to the spectrum of a reference gas (N_2O). A typical spectrum is displayed in Figure 2a.

The asymmetric C−O vibrational band of the dimer and monomer can be found within the same spectral region (see Figure 2) and are partially overlapping. Whereas the dimer is dominant in the supersonic expansion, the monomer transitions are also present. To come to an unambiguous assignment of all observed lines, we have carried out separate measurements of formic acid monomer by introducing a gas mixture of He−Ne and formic acid in the chamber at room temperature at low pressures. This allowed us to unambiguously distinguish between monomer and dimer transitions.

We were able to assign 309 lines to the C−O antisymmetric stretch vibrational band of FAD in the frequency range from

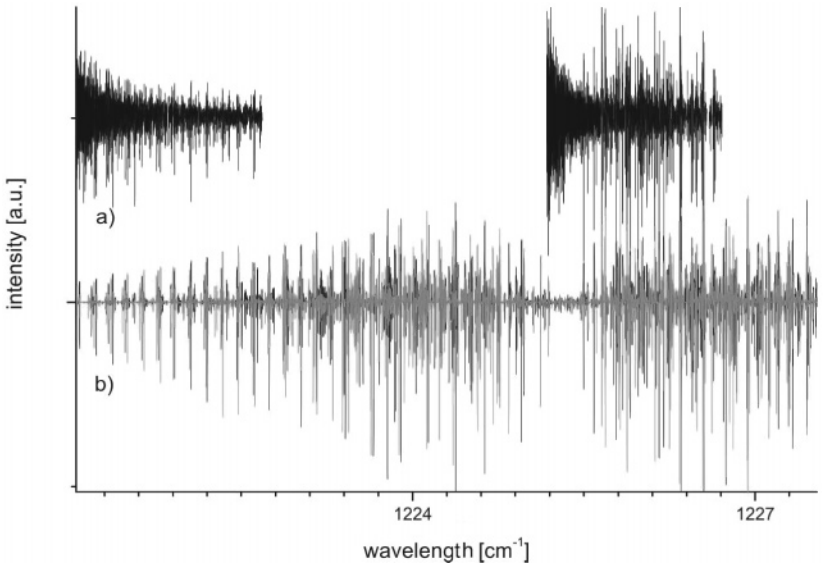

Figure 3. Spectrum of the ν_{C-O} band of $(HCOOH)_2$. Displayed is (a) the experimental spectrum and (b) the simulated spectrum based upon the vibrational−rotational parameters as obtained in the final fit.

TABLE 1: Spin Statistical Weights

G_8	D_{2h}	$(HCOOH)_2$
$A'_{1,2}$	$A_{g,u}$	1
$B''_{1,2}$	$B_{1g,1u}$	3
$B'_{1,2}$	$B_{2g,2u}$	3
$A''_{1,2}$	$B_{3g,3u}$	9

1221.0 to 1226.7 cm^{-1}. The restricted frequency coverage of our diodes resulted in frequency gaps in the experimental spectrum, as can be seen in Figure 3. We compare the spectrum as simulated from the final fitting parameter to the experimentally observed spectrum.

The intensities of the experimentally observed transitions resembles a population of the rotational states which follow a Boltzmann population. For the cw nozzle, the rotational temperature is found to be approximately 20 K; for the pulsed nozzle, the observed intensities are best described assuming lower rotational temperatures of ca. 10 K.

3. Analysis

A. Symmetries and Selection Rules. For FAD, a planar structure with C_{2h} symmetry was anticipated. When assuming a synchronous tunneling motion the molecular symmetry group corresponds to the permutation-inversion group G_8 which is isomorphic to D_{2h} (see ref 34 for further details). A detailed characterization of the different symmetries, and their spin statistical weights for $(DCOOH)_2$ can be found in ref 7. For $(HCOOH)_2$, the rotational−vibrational symmetries along with their spin statistical weights are given in Table 1.

The vibrational symmetry of the ground state and the vibrationally excited (antisymmetric C−O stretch vibration) state is A_g and B_u, respectively. FAD is an asymmetric rotor, the rotational levels are described by their quantum number J, K_a, and K_c. The symmetries for each rotational state are labeled according to the point group C_{2h}. In case tunneling is feasible, each vibrational−rotational level is split into two states (referred to as upper and lower tunneling level). The overall symmetry of each state in the molecular symmetry group G_8 is a product of the vibrational, rotational, and tunneling symmetries. They are displayed in Figure 4.

The electric dipole moment has A'_1 symmetry, which implies that the following transitions are allowed: $A'_1 \leftrightarrow A'_2$, $A''_1 \leftrightarrow A''_2$, $B'_1 \leftrightarrow B'_2$, and $B''_1 \leftrightarrow B''_2$.

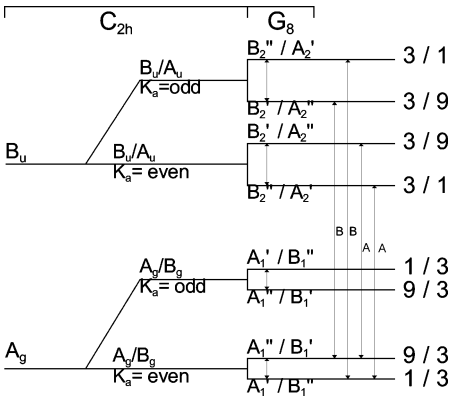

Figure 4. Energy level scheme for $(HCOOH)_2$ showing the symmetries of the vibrational−rotational tunneling states. The vibrational symmetries are A_g and B_u for $\nu_{C-O} = 0$ and $\nu_{C-O} = 1$, respectively. The symmetry of each rovibrational state is determined by K_a (first splitting), the tunneling state (second splitting), and whether K_c is even or odd (indicated, e.g., by A'_1/B''_1, respectively). At the right side, the corresponding spin statistical weights are given.

This implies that, for $(HCOOH)_2$, the proton transfer tunneling splittings in the ground and vibrationally excited states can be determined separately by measuring two types of transitions (a- and b-type transitions). a-type ($\Delta K_a = 0$) and b-type ($\Delta K_a = 1$) transitions describe a distinct reorientation of the angular momentum with respect to the axes of inertia of the molecule upon rovibrational excitation. As a consequence of the selection rules, b-type transitions involve a change of tunneling state upon vibrational excitation: The transition will go from the lower tunneling component to the upper tunneling component and vice versa. For a-type transitions, we find transitions from upper-to-upper and lower-to-lower tunneling component, as can be seen in Figure 4. By measuring both a- and b-type transitions, the sum and the difference of the tunneling splitting in the ground and vibrationally excited states can obtained independently.

The direction of the transition dipole moment for the infrared spectrum is given by the size of the projection of the derivative of the dipole moment for the C−O stretch onto the corresponding axis of the inertia ellipsoid. The change of the dipole moment during the antisymmetric C−O stretch for FAD is expected to have a projection along the intermolecular axis (*a*-axis) and

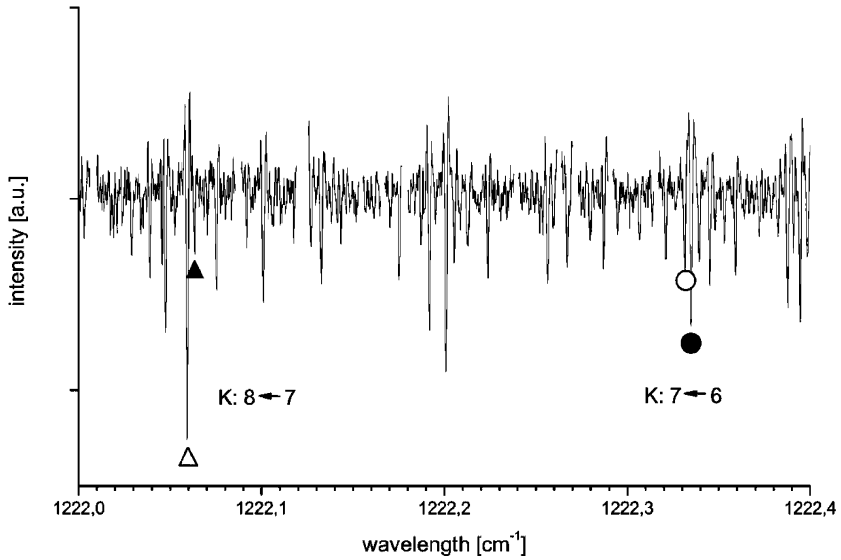

Figure 5. Part of the experimental spectrum. Marked are the R(9) transitions for K_a: 8 ← 7 and K_a: 7 ← 6. Both of them are split due to proton transfer tunneling.

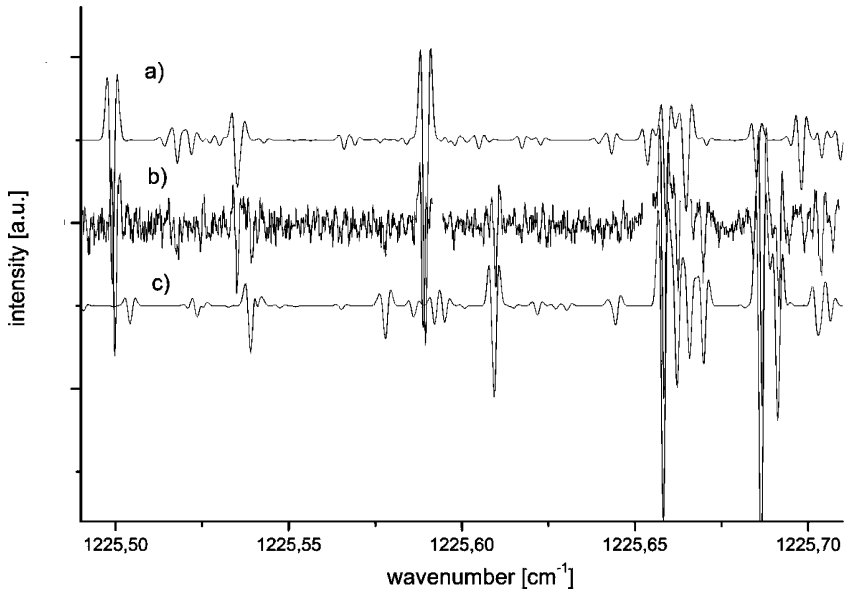

Figure 6. Part of the experimental spectrum (b) in direct comparison with simulated spectra (a,c). The simulated spectrum in the upper trace (a) shows the rovibrational spectrum of $(HCOOH)_2$ originating from a transition of the upper tunneling component of $\nu_{C-O} = 0$ to the lower tunneling component of $\nu_{C-O} = 1$. The lower trace (c) shows the simulation for the transition from the lower tunneling component for $\nu_{C-O} = 0$ to the upper tunneling component of $\nu_{C-O} = 1$

perpendicular to this (*b*-axis), with the later one being smaller. For a simulation of the spectrum, we assumed a ratio of 3:1 for the a-type compared to the b-type transition dipole moment, which resulted in good agreement between the predicted and the measured intensities.

For a P-branch with an unresolved K-type doubling, one expects an intensity-ratio of 1:3 for the two tunneling states. For K_a, even the spin statistical weight for the lower state tunneling is the sum of the weights of A_1' (1) and B_1''(3), which is 4, with the number in brackets corresponding to the spin statistical weights for each symmetry. The corresponding weight for the upper tunneling state is the sum of the weights of A_1'' (9) and B_1' (3), which is 12.

B. Assignment. In our previous study, we could show that the high-resolution spectroscopy using our lead salt diode laser spectrometer enables us to fully resolve the proton tunneling splitting for each rovibrational transition of $(DCOOH)_2$. The same was expected to hold for the present study because the tunneling splittings for $(HCOOH)_2$ should be in the same order of magnitude. In Figure 5, we display part of the spectrum in the frequency range from 1222.0 to 1222.4 cm^{-1}, where we show that each rotational vibrational transition is split into two fully resolved tunneling components.

We were able to assign 136 lines to b-type transitions from the upper tunneling state in the vibrational ground state to the lower tunneling state in the vibrationally excited state ν_{C-O}, hereby designated as (*l*) ← (*u*); 139 lines were attributed to b-type transitions, originating from the lower tunneling state to the upper tunneling state in the vibrationally excited state, hereby noted as (*u*) ← (*l*) transitions. In addition, we could assign 34 lines to a-type transitions, designated as (*u*) ← (*u*) or (*l*) ← (*l*). The observation of a-type transitions is facilitated by their smaller intensity. All transitions are listed in Table 4.

In Figure 6, we see that each of the marked rovibrational transition is split into two transitions originating from the two distinct tunneling states. According to the energy scheme in

TABLE 2: Fitted Molecular Constants for the Vibrational-Tunneling States of $(HCOOH)_2$

state	$E_l\nu_{C-O}=0$	$E_u\nu_{C-O}=0$	$E_l\nu_{C-O}=1$	$E_u\nu_{C-O}=1$
A[a]	0.20240(3)	0.20241(3)	0.20190(3)	0.20186(3)
B[a]	0.07623(2)	0.07645(2)	0.07575(2)	0.07552(2)
C[a]	0.05547(3)	0.05537(3)	0.05504(3)	0.05501(3)
D_j[b]	−3(8)	74(5)	106(7)	8(3)
D_{jk}[b]	81(2)	−55(2)	64(2)	98(2)
ν_0[a]	0	0.0158(4)	1225.3480(4)	1225.3380(2)
ΔI[amu]^2	−0,5078	0,7036	0,2188	−0,3054

[a] [cm^{-1}]. [b] [cm^{-8}].

TABLE 3: Experimentally Determined Tunneling Splitting in $(HCOOH)_2$

	tunneling splitting [cm^{-1}]	tunneling splitting [MHz]
ν_0	0.0158(4)	474(12))
ν_{C-O}	0.0100(3)	301(9)

Figure 4, we expect an intensity ratio of 9:1 and 3:3 between the two tunneling components depending on whether K_c is even or odd. However, as long as the K-type doubling remains unresolved (e.g., for $K_a \geq 7$), an intensity ratio of $(9+3)/(1+3) = 12/4$ is expected, in very good agreement with our experimental observation.

We were able to simultaneously fit all transitions within their experimental uncertainty using a standard rigid rotor Watson *S*-reduced Hamiltonian. The rotational parameters of each tunneling state could be determined independently. The result of the fit is summarized in Table 2.

By the assignment of b-type and a-type transitions, we were able to independently determine the tunneling splitting in the ground and vibrationally excited state. The results are summarized in Table 3.

It is interesting to note that, in the vibrationally excited state, the energy of the state that is labeled as lower tunneling state lies above the state that is labeled as upper tunneling state. However, the notation upper/lower just reflects the symmetries involved, e.g., for even K_a, the lower tunneling component has the symmetry B_2'' or A_2', depending on whether K_c is even or odd. The upper tunneling component has the symmetry B_2' or A_2'', depending on whether K_c is even or odd. In case that no perturbation is present, the upper tunneling component is expected to lie energetically above the lower tunneling component. However, due to the fact that the involved energy differences between the two tunneling states are very small, a coupling to a nearby state of the same symmetry can result in additional energy shifts, which can cause a switch in energy ordering. The observed change in the tunneling order as reported here can therefore be seen as a clear indication that the vibrationally excited state is perturbed by another nearby state, similar to what was observed before for the monomer. The fitted rotational constants are therefore only effective fitting parameters which prevent direct conclusion regarding the structure. A coupling to other vibrational states, which will result in effective rotational constants, has also been proposed by Luckhaus.[23]

4. Discussion

The vibrational frequency of the asymmetric C−O stretch was determined as $\nu_0 = 1225.3430(3)$ cm^{-1}, which deviates significantly from the values of the vibrational band center (1215 cm^{-1}), as given in the paper by Marechal.[24] The discrepancy can be explained by the fact that, in their paper, the vibrational band centers were determined at room temperature. In this case, hot bands contribute considerably to the observed low-resolution spectrum. In addition, combination bands can overlap with the fundamental band. In consequence, both effects will result in a blue-shift of the observed band center compared to the fundamental band, similar to what was found for $(DCOOH)_2$.[7]

In our previous publication, which reported the infrared spectroscopy of the ν_{C-O} vibrational band of $(DCOOH)_2$, we were unable to come to an unambiguous fit of the data.[7] Because of a lack of intensive a-type transitions and overlap with stronger lines in this frequency range, an assignment of these transitions to a specific tunneling component remained difficult. Therefore, two distinct assignments resulting in two different fits were given in the paper. Whereas a change in assignment did hardly affect the rotational constants, it did alter the size of the tunneling splittings: For the ground state tunneling splitting, either 0.00286(25) or 0.0123(3) cm^{-1} was obtained. For tunneling splitting in the vibrationally excited state ν_{C-O}, either 0.00999(21) or 0.0031(3) cm^{-1} was determined.

In our previous paper,[7] we favored the first assignment, which yielded an increase in the tunneling splitting upon vibrational excitation (e.g., 0.00286(25) cm^{-1} for the ground state and 0.00999(21) cm^{-1} for ν_{C-O}). It was argued that an acceleration of the proton transfer upon vibrational excitation seems more likely. This preference was based upon the fact that the vibrational analysis involves a mean decrease in the distance between the opposite O atoms of the two monomeric units. This was assumed to result in a lower reaction barrier for the double proton transfer, yielding a decrease of the proton transfer time and, consequently, an increase in the tunneling splitting. A similar enhancement of the tunneling splitting was predicted for malonaldehyde when the O−O stretching vibration was excited.[35] Experimentally it was found that OH bending/torsion motions decrease the tunneling splitting, some others leave it unchanged.[36]

Subsequent theoretical studies of Tautermann et al. yielded a value of 0.0022 cm^{-1} for the ground state, thereby supporting this initial assignment. In 2004 and 2005, direct dynamics calculation based on instanton techniques were reported, predicting the tunneling splittings of formic acid dimer and its deuterated isotopomers for the zero-point level and the lowest vibrationally excited level of a nontotally symmetric C−O stretch vibration.[37] The calculated splittings of Smerdarchina et al. are in good agreement with the experimental observations for $(DCOOH)_2$ with a yet reversed assignment, yielding experimental tunneling splittings of 0.0123(3) cm^{-1} for the ground state and 0.0031(3) cm^{-1} in the vibrationally excited state. In their paper, a deceleration upon vibrational excitation is attributed to the antisymmetric nature of the vibration, which handicaps a symmetrical proton transfer. The zero-point tunneling splitting of formic acid dimer is calculated to be 510 MHz, which is a factor of 1.4 larger than the observed splitting. This discrepancy is explained by the tendency of the B3LYP potential to underestimate the barrier height and width.

To a very good approximation, the tunneling splitting should be independent upon deuteration of the outer H atom. Because the energy levels in the upper state are obviously affected by perturbations, we will restrict a direct comparison with the previous results for $(DCOOH)_2$ to the unperturbed ground state. The tunneling splitting of $(HCOOH)_2$ in the ground state amounts to 0.0158(4) cm^{-1}, which is in close agreement with the value of 0.0123(3) cm^{-1} for $(DCOOH)_2$ for the reversed assignment, thereby strongly supporting the second alternative assignment. We want to add that this result is also in agreement with new theoretical predictions by Matanović et al. by density functional theory using a B3LYP functional.[38]

TABLE 4: Observed A-Type Transitions : $\nu_{C-O} = 1 \leftarrow 0$; Lower ← Lower

V	J_{up}	K_A	K_C	V	J_l	K_A	K_C	obs freq	calc freq	obs − calc	V	J_{up}	K_A	K_C	V	J_l	K_A	K_C	obs freq	calc freq	obs − calc
2	8	5	3	0	8	5	4	1221.1884	1221.1877	0.00074	3	6	2	5	0	7	1	6	1222.5308	1222.5304	0.00044
2	9	5	5	0	9	5	4	1221.2111	1221.2104	0.00068	3	10	2	9	0	9	1	8	1222.5406	1222.5392	0.00142
2	6	3	3	0	6	3	4	1221.2288	1221.2288	0.00001	3	11	2	9	0	11	1	10	1222.5863	1222.5851	0.00120
2	3	3	1	0	3	3	0	1221.3359	1221.3357	0.00017	3	13	4	9	0	14	5	10	1222.6062	1222.6041	0.00214
2	5	1	5	0	4	1	4	1221.3582	1221.3577	0.00046	3	4	2	3	0	3	1	2	1222.6062	1222.6069	−0.00067
2	11	9	3	0	11	9	2	1221.4829	1221.4827	0.00021	3	4	2	3	0	4	1	4	1222.6182	1222.6178	0.00036
2	7	7	1	0	7	7	0	1221.6284	1221.6285	−0.00012	3	9	4	5	0	9	3	6	1224.5679	1224.5685	−0.00064
2	3	1	3	0	2	1	2	1221.6483	1221.6486	−0.00025	3	9	2	7	0	9	3	6	1224.5764	1224.5764	0.00002
2	10	5	5	0	10	5	6	1221.7567	1221.7559	0.00082	3	2	2	1	0	1	1	0	1224.5934	1224.5925	0.00087
2	8	7	1	0	8	7	2	1221.7729	1221.7732	−0.00033	3	5	3	2	0	4	2	3	1224.6872	1224.6860	0.00119
2	4	3	1	0	4	3	2	1221.7916	1221.7920	−0.00043	3	3	2	1	0	2	1	2	1224.7016	1224.7038	−0.00222
2	7	5	3	0	7	5	2	1221.9028	1221.9021	0.00073	3	8	1	8	0	7	0	7	1224.7386	1224.7376	0.00097
2	6	4	2	0	6	4	3	1222.0475	1222.0473	0.00016	3	11	4	7	0	11	3	8	1224.7458	1224.7454	0.00038
2	9	7	3	0	9	7	2	1222.0592	1222.0592	−0.00001	3	13	6	8	0	13	5	9	1224.7633	1224.7630	0.00027
2	9	9	1	0	9	9	0	1222.1918	1222.1916	0.00018	3	11	2	10	0	10	1	9	1224.7662	1224.7657	0.00051
2	5	5	1	0	5	5	0	1222.3348	1222.3348	−0.00005	3	2	1	2	0	3	0	3	1224.9758	1224.9749	0.00090
2	6	5	1	0	6	5	2	1222.4768	1222.4769	−0.00014	3	12	4	9	0	12	3	10	1225.1230	1225.1223	0.00069
3	5	4	1	1	5	4	2	1222.6132	1222.6127	0.00050	3	6	2	4	0	6	1	5	1225.5000	1225.4991	0.00091
3	10	10	1	1	10	10	0	1224.9082	1224.9064	0.00179	3	7	4	3	0	7	3	4	1225.5354	1225.5350	0.00040
3	3	2	1	1	3	2	2	1224.9143	1224.9126	0.00168	3	8	2	6	0	8	1	7	1225.5890	1225.5896	−0.00060
3	9	8	1	1	9	8	2	1225.2687	1225.2714	−0.00274	3	8	5	3	0	8	4	4	1225.6099	1225.6093	0.00057
3	5	2	3	1	4	2	2	1225.2991	1225.2993	−0.00023	3	6	4	3	0	6	3	4	1225.6586	1225.6582	0.00042
3	8	4	5	1	8	4	4	1225.3397	1225.3403	−0.00062	3	7	1	6	0	7	0	7	1225.6625	1225.6622	0.00030
3	7	6	1	1	7	6	2	1225.7013	1225.7051	−0.00382	3	5	0	5	0	4	1	4	1225.6697	1225.6699	−0.00015
3	9	6	3	1	9	6	4	1225.8339	1225.8351	−0.00117	3	4	4	1	0	4	3	2	1225.6870	1225.6864	0.00058
3	6	6	1	1	6	6	0	1225.8440	1225.8439	0.00015	3	10	3	8	0	10	2	9	1225.6917	1225.6913	0.00045
3	8	8	1	1	8	8	0	1225.9319	1225.9318	0.00011	3	7	3	4	0	7	2	5	1225.7330	1225.7340	−0.00099
3	8	6	3	1	8	6	2	1225.9949	1225.9947	0.00022	3	4	2	2	0	4	1	3	1225.7595	1225.7606	−0.00110
3	3	0	3	1	2	0	2	1226.0042	1226.0044	−0.00022	3	7	4	4	0	7	3	5	1225.7837	1225.7834	0.00030
3	10	8	3	1	10	8	2	1226.1233	1226.1258	−0.00253	3	13	3	10	0	13	2	11	1225.7971	1225.7968	0.00030
3	3	2	1	1	2	2	0	1226.2003	1226.1990	0.00130	3	8	4	4	0	8	3	5	1225.8065	1225.8060	0.00045
3	4	4	1	1	4	4	0	1226.2708	1226.2699	0.00093	3	11	4	8	0	11	3	9	1225.8214	1225.8206	0.00081
3	5	0	5	1	4	0	4	1226.4319	1226.4320	−0.00015	3	9	2	8	0	8	1	7	1225.8417	1225.8436	−0.00191
3	4	2	3	1	3	2	2	1226.5040	1226.5027	0.00129	3	8	5	4	0	8	4	5	1225.8665	1225.8669	−0.00036
3	7	6	2	0	8	7	1	1221.0845	1221.0838	0.00074	3	7	5	2	0	7	4	3	1225.8665	1225.8669	−0.00041
3	9	6	4	0	10	7	3	1221.0869	1221.0865	0.00045	3	12	5	7	0	12	4	8	1225.8800	1225.8797	0.00027
3	8	6	3	0	9	7	2	1221.2317	1221.2326	−0.00089	3	4	0	4	0	5	1	5	1225.8934	1225.8931	0.00027
3	3	0	3	0	3	1	2	1221.3174	1221.3187	−0.00127	3	13	6	7	0	13	5	8	1225.8998	1225.9019	−0.00213
3	7	0	7	0	7	1	6	1221.3555	1221.3560	−0.00048	3	8	4	5	0	8	3	6	1225.9076	1225.9065	0.00108
3	7	2	5	0	7	3	4	1221.3722	1221.3725	−0.00032	3	9	2	7	0	8	3	6	1225.9525	1225.9527	−0.00022
3	6	2	5	0	6	1	6	1221.3767	1221.3774	−0.00069	3	2	1	2	0	1	0	1	1225.9525	1225.9530	−0.00048
3	9	5	4	0	10	6	5	1221.3921	1221.3934	−0.00128	3	1	1	0	0	1	0	1	1225.9797	1225.9785	0.00123
3	9	8	2	0	10	9	1	1221.4829	1221.4825	0.00039	3	15	5	11	0	15	4	12	1225.9917	1225.9901	0.00162
3	5	0	5	0	6	1	6	1221.5005	1221.5009	−0.00042	3	3	1	2	0	3	0	3	1225.9976	1225.9973	0.00032
3	8	2	7	0	8	1	8	1221.5034	1221.5038	−0.00039	3	4	1	4	0	3	0	3	1226.0107	1226.0121	−0.00139
3	5	2	3	0	5	1	4	1221.5516	1221.5507	0.00087	3	13	2	11	0	13	1	12	1226.0107	1226.0096	0.00109
3	11	4	7	0	12	5	8	1221.5673	1221.5670	0.00031	3	2	2	1	0	2	1	2	1226.0184	1226.0184	−0.00005
3	9	2	7	0	9	1	8	1221.6082	1221.6101	−0.00190	3	10	2	9	0	10	1	10	1226.0312	1226.0316	−0.00043
3	8	8	1	0	9	9	0	1221.6300	1221.6294	0.00055	3	10	1	10	0	9	0	9	1226.0342	1226.0340	0.00018
3	5	2	3	0	5	3	2	1221.6445	1221.6446	−0.00012	3	5	4	2	0	5	3	3	1226.0519	1226.0532	−0.00126
3	7	2	5	0	7	1	6	1221.6556	1221.6558	−0.00019	3	15	4	11	0	15	3	12	1226.0754	1226.0749	0.00051
3	11	8	4	0	12	9	3	1221.7567	1221.7568	−0.00006	3	5	1	4	0	5	2	3	1226.0813	1226.0806	0.00074
3	12	6	7	0	13	7	6	1221.7759	1221.7753	0.00064	3	4	1	4	0	5	0	5	1226.0830	1226.0833	−0.00031
3	3	0	3	0	4	1	4	1221.7871	1221.7871	0.00001	3	8	3	6	0	8	2	7	1226.0963	1226.0984	−0.00205
3	8	5	4	0	9	6	3	1221.8813	1221.8816	−0.00030	3	7	1	7	0	6	0	6	1226.1023	1226.1017	0.00061
3	12	8	5	0	13	9	4	1221.9012	1221.9019	−0.00066	3	10	4	6	0	10	3	7	1226.1362	1226.1358	0.00037
3	9	7	3	0	10	8	2	1221.9164	1221.9168	−0.00039	3	10	0	10	0	9	1	9	1226.1738	1226.1725	0.00132
3	11	6	6	0	12	7	5	1221.9198	1221.9199	−0.00010	3	7	1	6	0	7	2	5	1226.1790	1226.1783	0.00073
3	12	7	6	0	13	8	5	1222.0291	1222.0301	−0.00101	3	7	2	6	0	6	1	5	1226.1865	1226.1863	0.00021
3	11	7	5	0	12	8	4	1222.0389	1222.0407	−0.00179	3	10	4	7	0	10	3	8	1226.2003	1226.1989	0.00140
3	10	9	1	0	11	10	2	1222.0457	1222.0460	−0.00033	3	6	3	4	0	6	2	5	1226.2003	1226.2002	0.00007
3	10	6	5	0	11	7	4	1222.0635	1222.0633	0.00018	3	3	0	3	0	2	1	2	1226.2239	1226.2239	−0.00003
3	10	8	2	0	11	9	3	1222.1752	1222.1757	−0.00054	3	14	5	10	0	14	4	11	1226.2283	1226.2289	−0.00063
3	11	9	2	0	12	10	3	1222.1874	1222.1892	−0.00183	3	14	4	10	0	14	3	11	1226.2347	1226.2331	0.00155
3	12	1	12	0	11	0	11	1222.2008	1222.2005	0.00033	3	12	2	11	0	12	1	12	1226.2461	1226.2458	0.00026
3	3	2	1	0	3	1	2	1222.2053	1222.2055	−0.00020	3	5	2	4	0	4	1	3	1226.2492	1226.2491	0.00017
3	7	7	0	0	8	8	1	1222.2670	1222.2666	0.00037	3	6	1	6	0	5	0	5	1226.2492	1226.2484	0.00083
3	6	6	0	0	7	7	1	1222.2869	1222.2860	0.00094	3	5	1	4	0	5	0	5	1226.2552	1226.2548	0.00044
3	9	9	0	0	10	10	1	1222.3208	1222.3196	0.00119	3	18	4	14	0	18	3	15	1226.2552	1226.2562	−0.00104
3	11	2	9	0	11	3	8	1222.3208	1222.3213	−0.00049	3	4	0	4	0	4	1	3	1226.2581	1226.2561	0.00197
3	8	7	2	0	9	8	1	1222.3314	1222.3314	−0.00004	3	9	0	9	0	8	1	8	1226.2607	1226.2600	0.00067
3	6	2	5	0	6	3	4	1222.4342	1222.4342	0.00001	3	9	1	8	0	9	0	9	1226.2628	1226.2629	−0.00011
3	12	4	9	0	13	5	8	1222.4624	1222.4623	0.00010	3	13	5	8	0	13	4	9	1226.2670	1226.2667	0.00028
3	15	6	9	0	16	7	10	1222.4646	1222.4629	0.00173	3	11	0	11	0	10	1	10	1226.2708	1226.2713	−0.00046
3	6	2	5	0	5	1	4	1222.4646	1222.4646	−0.00003	3	5	0	5	0	5	1	4	1226.2789	1226.2787	0.00022
3	10	7	4	0	11	8	3	1222.4727	1222.4726	0.00009	3	8	0	8	0	7	1	7	1226.2819	1226.2802	0.00166
3	13	6	7	0	14	7	8	1222.4929	1222.4919	0.00100	3	6	4	2	0	6	3	3	1226.2847	1226.2846	0.00012
3	6	2	5	0	7	1	6	1222.5308	1222.5304	0.00044	3	11	2	9	0	10	3	8	1226.2864	1226.2863	0.00012

TABLE 4 (Continued)

V	J_{up}	K_A	K_C	V	J_l	K_A	K_C	obs freq	calc freq	obs − calc	V	J_{up}	K_A	K_C	V	J_l	K_A	K_C	obs freq	calc freq	obs − calc
3	5	3	2	0	5	2	3	1226.3593	1226.3591	0.00022	2	5	1	5	1	4	0	4	1225.7038	1225.7037	0.00010
3	4	0	4	0	3	1	3	1226.3872	1226.3880	−0.00080	2	15	5	11	1	15	4	12	1225.7173	1225.7191	−0.00177
3	9	4	6	0	9	3	7	1226.4033	1226.4029	0.00041	2	7	3	5	1	7	2	6	1225.7353	1225.7350	0.00027
3	4	2	3	0	4	3	2	1226.4056	1226.4055	0.00011	2	13	7	7	1	14	8	6	1225.7433	1225.7437	−0.00042
3	9	3	6	0	9	2	7	1226.4445	1226.4442	0.00026	2	9	8	2	1	10	9	1	1225.7477	1225.7474	0.00029
3	5	4	1	0	5	3	2	1226.4823	1226.4835	−0.00117	2	8	8	0	1	9	9	1	1225.7746	1225.7754	−0.00083
3	11	5	6	0	12	6	7	1226.5250	1226.5251	−0.00014	2	11	3	9	1	12	4	8	1225.7929	1225.7921	0.00078
3	10	2	8	0	10	3	7	1226.5382	1226.5383	−0.00006	2	10	4	6	1	10	3	7	1225.7972	1225.7956	0.00155
3	6	0	6	0	5	1	5	1226.5445	1226.5454	−0.00085	2	18	3	15	1	19	4	16	1225.8004	1225.7996	0.00081
3	8	2	7	0	7	1	6	1226.5532	1226.5532	0.00001	2	5	0	5	1	6	1	6	1225.8007	1225.7992	0.00154
3	10	2	9	0	9	3	6	1226.5637	1226.5630	0.00069	2	12	3	9	1	11	4	8	1225.8625	1225.8616	0.00098
3	11	3	8	0	11	2	9	1226.6073	1226.6077	−0.00035	2	5	1	5	1	5	2	4	1225.8722	1225.8712	0.00100
3	13	4	9	0	13	3	10	1226.6216	1226.6212	0.00035	2	12	2	10	1	12	1	11	1225.8772	1225.8767	0.00048
3	8	2	6	0	8	3	5	1226.6370	1226.6373	−0.00028	2	5	1	4	1	5	0	5	1225.8772	1225.8772	0.00000
3	5	2	3	0	4	1	4	1226.6446	1226.6470	−0.00234	2	10	2	8	1	10	1	9	1225.8801	1225.8804	−0.00027
3	7	0	7	0	6	1	6	1226.6759	1226.6764	−0.00052	2	11	5	7	1	11	4	8	1225.8883	1225.8882	0.00006
3	3	2	2	0	2	1	1	1226.6799	1226.6799	0.00003	2	5	1	4	1	5	2	3	1225.8908	1225.8920	−0.00120
3	11	4	7	0	10	5	6	1226.6969	1226.6956	0.00127	2	9	5	5	1	9	4	6	1225.9079	1225.9073	0.00057
2	12	3	9	1	12	2	10	1222.1791	1222.1797	−0.00056	2	10	1	10	1	9	0	9	1225.9101	1225.9103	−0.00020
2	10	1	9	1	10	2	8	1224.5676	1224.5677	−0.00014	2	8	5	3	1	8	4	4	1225.9225	1225.9247	−0.00216
2	4	3	2	1	3	2	1	1224.5874	1224.5886	−0.00116	2	19	3	16	1	20	4	17	1225.9416	1225.9436	−0.00202
2	10	0	10	1	9	1	9	1224.6295	1224.6311	−0.00161	2	10	5	5	1	11	6	6	1225.9475	1225.9474	0.00014
2	7	1	7	1	7	2	6	1224.6331	1224.6321	0.00106	2	14	7	8	1	15	8	7	1225.9767	1225.9767	−0.00002
2	15	5	10	1	16	6	11	1224.6373	1224.6362	0.00106	2	10	2	8	1	10	3	7	1225.9835	1225.9836	−0.00015
2	6	1	6	1	5	0	5	1224.6667	1224.6684	−0.00175	2	10	6	5	1	11	7	4	1226.0020	1226.0021	−0.00006
2	5	3	2	1	4	2	3	1224.7426	1224.7424	0.00018	2	9	1	8	1	8	2	7	1226.0039	1226.0042	−0.00034
2	6	3	4	1	6	2	5	1224.7446	1224.7446	0.00002	2	8	1	7	1	8	0	8	1226.0153	1226.0143	0.00101
2	16	5	11	1	17	6	12	1224.7456	1224.7467	−0.00108	2	10	9	1	1	11	10	2	1226.0663	1226.0663	0.00004
2	11	8	4	1	12	9	3	1224.7568	1224.7577	−0.00092	2	9	7	3	1	10	8	2	1226.0702	1226.0698	0.00038
2	8	1	7	1	8	2	6	1224.7663	1224.7661	0.00016	2	4	1	3	1	4	2	2	1226.0703	1226.0697	0.00060
2	4	3	1	1	4	2	2	1224.7705	1224.7698	0.00075	2	17	4	13	1	17	3	14	1226.0777	1226.0752	0.00247
2	11	1	10	1	10	2	9	1224.8418	1224.8445	−0.00268	2	8	3	5	1	8	2	6	1226.1052	1226.1047	0.00057
2	4	1	3	1	4	0	4	1224.9194	1224.9182	0.00119	2	10	3	7	1	10	2	8	1226.1233	1226.1218	0.00154
2	7	1	7	1	6	0	6	1224.9492	1224.9482	0.00097	2	8	0	8	1	7	1	7	1226.1461	1226.1453	0.00079
2	11	1	11	1	10	0	10	1224.9566	1224.9552	0.00144	2	12	7	6	1	13	8	5	1226.1591	1226.1588	0.00026
2	8	2	6	1	8	1	7	1224.9661	1224.9651	0.00107	2	4	1	4	1	5	0	5	1226.1624	1226.1615	0.00098
2	6	5	1	1	6	4	2	1224.9753	1224.9750	0.00029	2	8	1	7	1	7	2	6	1226.1820	1226.1819	0.00008
2	10	1	9	1	10	0	10	1224.9768	1224.9763	0.00045	2	11	6	6	1	12	7	5	1226.2305	1226.2322	−0.00170
2	5	3	3	1	5	2	4	1224.9789	1224.9795	−0.00055	2	12	6	7	1	13	7	6	1226.2305	1226.2314	−0.00087
2	5	1	5	1	6	0	6	1225.0554	1225.0567	−0.00135	2	11	4	7	1	11	3	8	1226.2492	1226.2498	−0.00058
2	2	1	1	1	2	0	2	1225.0602	1225.0599	0.00036	2	3	1	2	1	3	0	3	1226.3163	1226.3166	−0.00033
2	8	4	4	1	8	3	5	1225.2513	1225.2510	0.00022	2	11	7	5	1	12	8	4	1226.3409	1226.3401	0.00078
2	11	3	8	1	11	2	9	1225.2540	1225.2528	0.00118	2	3	1	3	1	2	0	2	1226.3471	1226.3474	−0.00026
2	9	3	7	1	8	4	4	1225.2660	1225.2659	0.00005	2	7	3	4	1	7	2	5	1226.3544	1226.3539	0.00050
2	9	3	6	1	9	2	7	1225.2664	1225.2657	0.00075	2	4	1	4	1	3	0	3	1226.3544	1226.3553	−0.00097
2	9	5	4	1	9	4	5	1225.2776	1225.2776	−0.00002	2	11	9	2	1	12	10	3	1226.3544	1226.3523	0.00213
2	13	5	9	1	13	4	10	1225.2778	1225.2773	0.00053	2	14	3	11	1	14	2	12	1226.4111	1226.4121	−0.00099
2	5	2	4	1	5	1	5	1225.2803	1225.2802	0.00004	2	9	9	0	1	10	10	1	1226.4211	1226.4210	0.00012
2	11	0	11	1	10	1	10	1225.2876	1225.2884	−0.00082	2	12	5	7	1	13	6	8	1226.4259	1226.4262	−0.00026
2	10	5	6	1	10	4	7	1225.2879	1225.2877	0.00020	2	1	1	1	1	0	0	0	1226.4261	1226.4289	−0.00276
2	12	4	8	1	12	3	9	1225.2965	1225.2970	−0.00054	2	6	2	4	1	6	1	5	1226.4261	1226.4272	−0.00105
2	5	3	2	1	5	2	3	1225.3018	1225.3038	−0.00196	2	10	5	6	1	11	6	5	1226.4346	1226.4348	−0.00018
2	9	2	8	1	8	1	7	1225.3044	1225.3020	0.00237	2	13	3	11	1	13	2	12	1226.4444	1226.4439	0.00050
2	12	2	10	1	11	3	9	1225.3049	1225.3048	0.00007	2	8	6	3	1	9	7	2	1226.4497	1226.4510	−0.00128
2	3	1	3	1	4	0	4	1225.3107	1225.3103	0.00035	2	8	5	4	1	9	6	3	1226.4502	1226.4498	0.00046
2	6	6	0	1	7	7	1	1225.3112	1225.3109	0.00033	2	4	0	4	1	3	1	3	1226.4503	1226.4509	−0.00057
2	6	2	5	1	5	1	4	1225.3126	1225.3122	0.00041	2	7	6	2	1	8	7	1	1226.4556	1226.4547	0.00087
2	7	2	5	1	7	1	6	1225.3186	1225.3197	−0.00114	2	15	4	12	1	15	3	13	1226.4557	1226.4571	−0.00148
2	5	0	5	1	4	1	4	1225.3217	1225.3207	0.00101	2	9	5	5	1	10	6	4	1226.4606	1226.4602	0.00037
2	13	4	10	1	13	3	11	1225.3267	1225.3261	0.00061	2	11	5	7	1	12	6	6	1226.4761	1226.4764	−0.00036
2	7	1	6	1	7	0	7	1225.3267	1225.3275	−0.00076	2	13	5	9	1	14	6	8	1226.4793	1226.4805	−0.00121
2	7	2	6	1	6	1	5	1225.3269	1225.3272	−0.00032	2	3	3	0	1	2	2	1	1226.4895	1226.4894	0.00005
2	11	2	10	1	10	1	9	1225.3326	1225.3332	−0.00059	2	4	3	1	1	3	2	2	1226.4929	1226.4926	0.00030
2	7	1	6	1	7	2	5	1225.3373	1225.3394	−0.00212	2	3	1	2	1	3	2	1	1226.5044	1226.5054	−0.00103
2	9	3	7	1	9	2	8	1225.3398	1225.3419	−0.00214	2	6	0	6	1	5	1	5	1226.5098	1226.5100	−0.00024
2	9	1	9	1	8	0	8	1225.4715	1225.4729	−0.00141	2	15	5	11	1	16	6	10	1226.5197	1226.5206	−0.00095
2	7	7	0	1	8	8	1	1225.4840	1225.4836	0.00040	2	12	0	12	1	11	1	11	1226.5224	1226.5223	0.00005
2	9	5	4	1	10	6	5	1225.5176	1225.5178	−0.00020	2	12	5	8	1	13	6	7	1226.5300	1226.5310	−0.00097
2	10	4	7	1	11	5	6	1225.5387	1225.5391	−0.00033	2	2	1	1	1	2	2	0	1226.5445	1226.5461	−0.00161
2	3	3	1	1	2	2	0	1225.5771	1225.5778	−0.00067	2	8	7	2	1	9	8	1	1226.5498	1226.5497	0.00007
2	5	3	3	1	4	2	2	1225.5793	1225.5782	0.00112	2	8	3	5	1	7	4	4	1226.5499	1226.5486	0.00125
2	7	5	3	1	7	4	4	1225.5890	1225.5891	−0.00012	2	10	1	9	1	9	2	8	1226.6320	1226.6324	−0.00038
2	10	5	5	1	10	4	6	1225.6582	1225.6590	−0.00077	2	9	6	4	1	10	7	3	1226.6471	1226.6460	0.00111
2	10	7	4	1	11	8	3	1225.6648	1225.6658	−0.00097	2	6	3	3	1	6	2	4	1226.6494	1226.6479	0.00156
2	12	1	12	1	11	0	11	1225.6652	1225.6652	−0.00002	2	16	5	12	1	17	6	11	1226.6665	1226.6663	0.00027
2	6	1	5	1	6	2	4	1225.6870	1225.6850	0.00197	2	10	8	3	1	11	9	2	1226.6855	1226.6853	0.00023
2	14	5	9	1	14	4	10	1225.6990	1225.7010	−0.00201	2	6	1	5	1	6	0	6	1226.6939	1226.6921	0.00182

However, it has become obvious now that the parameters in the upper state, including the tunneling splitting, can only be regarded as effective parameters. Therefore, we cannot draw any further conclusion regarding an acceleration or decelaration of proton transfer tunneling upon excitation of the C−O stretch.

5. Summary

We have observed the ν_{C-O} vibration of the formic acid dimer in direct absorption around 1225.3 cm^{-1}. High-resolution spectroscopy allows an exact quantitative measurement of important dynamical processes. The tunneling motion in carboxylic dimers is shown to be slow compared to the overall rotation, thus confirming the existence of deep local minima in a C_{2h} structure. The proton transfer time of formic acid dimer in the gas phase has been determined to be 1.0 ns. This experimental data can be directly compared to recent theoretical predictions. The measured tunneling splittings in $(HCOOH)_2$ favor a reversed assignment of the spectrum of the corresponding vibrational band of $(DCOOH)_2$ as reported previously.[7]

The exact knowledge of the proton transfer in carboxylic dimers constitutes an important benchmark system for theoretical models describing hydrogen transfer in double hydrogen-bonded dimers. This is considered to be an important issue for the future because, as long as we have not tested the reliability of theoretical models on simple benchmark systems, we probably will not be able to quantitatively simulate proton transfer tunneling in biological systems in the future.

Acknowledgment. We thank Erik Bründermann for his help with the asymmetric fitting programme. This work has been supported by the Deutsche Forschungsgemeinschaft (DFG) by the project Ha2394/13-1 within the Forschergruppe 618.

References and Notes

(1) Gantenberg, M.; Halupka, M.; Sander, W. *Chem.—Eur. J.* **2000**, *6*, 1865.
(2) Robertson, G. N.; and Lawrence, M. C. *Chem. Phys.* **1981**, *62*, 131.
(3) Scheele, I.; Lehnig, R.; Havenith, M. *Mol. Phys.* **2001**, *99*, 205.
(4) Bunker, P. R.; Jensen, P. *Molecular Syrnmetry and Spectroscopy*, 2nd ed.; National Research Council of Canada Press: Ottawa, 1998.
(5) Almeningen, A.; Bastiansen, O.; Motzfeld, T. *Acta. Chem. Scand.* **1969**, *23*, 2848.
(6) Jursic, B. S. *J. Mol. Struct.* **1997**, *417*, 89.
(7) Madeja, F.; Havenith, M. *J. Chem. Phys.* **2002**, *117*, 7162.
(8) Matylitsky, V. V.; Riehn, C.; Gelin, M. F.;Brutschy, B. *J. Chem. Phys.* **2003**, *119*, 10553.
(9) Neuheusser, Th.; Hess, B. A.; Reutel, Ch.; Weber, E. *J. Phys. Chem.* **1994**, *98*, 6459.
(10) Miura, Sh.; Tuckermann, M. E.; and Klein, M. L. *J. Chem. Phys.* **1998**, *109*, 5290.
(11) Jursic, B. S. *J. Am. Chem. Soc.* **1995**, *118*, 1522.
(12) Madeja, F.; Havenith, M.; Nauta, K.; Miller, R. E.; Chocholoušová, J.; Hobza, P. *J. Chem. Phys.* **2004**, *120*, 10554.
(13) Shida, N.; Barbara, P. E.; Almlöf, W J. *J. Chem. Phys.* **1991**, *94*, 3633.
(14) Wolf, K.; Simperler, A.; and Mikenda, W.; Monatsh. *Chem.* **1999**, *130*, 1031.
(15) Markwick, P. R. L.; Doltsinis, N. L.; Marx, D. *J. Chem. Phys.* **2005**, *122*, 054112-1.
(16) Filleaux, F. *Chem. Phys. Lett.* **2005**, *408*, 302.
(17) Chang, Y.-T.; Yamaguchi, Y.; Miller, W. H.; Schaeffer, F., III. *J. Am. Chem. Soc.* **1987**, *109*, 7247.
(18) Ushiyama, H.; Takatsuka, K. *J. Chem. Phys.* **2001**, *115*, 5903.
(19) Vener, M. V.; Kuhn, O.; Bowman, J. M. *Chem. Phys. Lett.* **2001**, *349*, 562.
(20) Chapter Tautermann, S.; Voegele, A. F.; Liedl, K. R. *J. Chem. Phys.* **2004**, *120*, 631.
(21) Smedarchina, Z.; Fernandez-Ramos, A.; Siebrand, W. *J. Chem. Phys.* **2005**, *122*, 134309.
(22) Milnikov, G. V.; Kuhn, O.; Nakamura, H. *J. Chem. Phys.* **2005**, *123*, 074308.
(23) Luckhaus, D. *J. Phys. Chem. A* **2006**, *110*, 3151.
(24) Marechal, Y. *J. Chem. Phys.* **1987**, *87*, 6344.
(25) Merker, U.; Engels, P.; Madeja, F.; Havenith, M.; Urban, W. *Rev. Sci. Instrum.* **1999**, *70*, 1933.
(26) Goh, K. L.; Ong, P. P.; Tan, T. L. *Spectrochim. Acta A.* **1999**, *55*, 2601.
(27) Wachs, T.; Borchardt, D.; Bauer, S. H. *Spectrochim. Acta A.* **1987**, *43*, 965.
(28) Bertie, J. E.; Michaelian, K. H.; Eysel, H. H.; Hager, D. J. *J. Chem. Phys.* **1986**, *85*, 4779.
(29) Millikan, R. C.; Pitzer, K. S. *J. Am. Chem. Soc.* **1958**, *80*, 3515.
(30) Georges, R.; Freytes, M.; Hurtmans, D.; Kleiner, I. Van der Auwera, J.; Herman, M. *J. Chem. Phys.* **2004**, *305*, 187.
(31) Florio, G. M.; Zwier, T.; Myshakin, E. M.; Jordan, K. D.; Sibert, E. L., III. *J. Chem. Phys.* **2003**, *118*, 1735.
(32) Havenith, M.; Hilpert, G.; Petri, M.; Urban, W. *Mol. Phys.* **1994**, *81*, 1003.
(33) König, S.; Hipert, G.; Havenith, M. *Mol. Phys.* **1995**, *86*, 1233.
(34) Ito, F.; Nakanaga, T. *J. Chem. Phys.* **2002**, *277*, 163.
(35) Sato, N.; Iwata, S. *J. Chem. Phys.* **1988**, *89*, 2932.
(36) Wassermann, T. N.; Luckhaus, D.; Coussan, S.; Suhm, M. A. *Phys. Chem. Chem. Phys.* **2006**, *8*, 2344.
(37) Smedarchina, Z.; Fernandez-Ramos, A.; and Siebrand, W. *Chem. Phys.* 2004.
(38) Matanović, I.; Došlić, N.; Kühn, O. private communication.